PHYSICAL REVIEW E **95**, 020101(R) (2017)

Interplay of interfacial noise and curvature-driven dynamics in two dimensions

Parna Roy and Parongama Sen
Department of Physics, University of Calcutta, 92 Acharya Prafulla Chandra Road, Kolkata 700009, India
(Received 22 November 2016; published 7 February 2017)

We explore the effect of interplay of interfacial noise and curvature-driven dynamics in a binary spin system. An appropriate model is the generalized two-dimensional voter model proposed earlier [M. J. de Oliveira, J. F. F. Mendes, and M. A. Santos, J. Phys. A: Math. Gen. **26**, 2317 (1993)], where the flipping probability of a spin depends on the state of its neighbors and is given in terms of two parameters, x and y. $x = 0.5$ and $y = 1$ correspond to the conventional voter model which is purely interfacial noise driven, while $x = 1$ and $y = 1$ correspond to the Ising model, where coarsening is fully curvature driven. The coarsening phenomena for $0.5 < x < 1$ keeping $y = 1$ is studied in detail. The dynamical behavior of the relevant quantities show characteristic differences from both $x = 0.5$ and 1. The most remarkable result is the existence of two time scales for $x \geqslant x_c$ where $x_c \approx 0.7$. On the other hand, we have studied the exit probability which shows Ising-like behavior with a universal exponent for any value of $x > 0.5$; the effect of x appears in altering the value of the parameter occurring in the scaling function only.

DOI: 10.1103/PhysRevE.95.020101

Nonequilibrium phenomena associated with the zero temperature ordering process in classical Ising and voter models [1–4] have been extensively studied in the recent past. Both models are two state models and the states can be represented by Ising spins. There is, however, a basic difference. The Ising model (IM) is defined using an energy function ($H = -J\sum \sigma_i\sigma_j$, where $\sigma = \pm 1$ and the sum is usually over nearest neighbors) and it has no intrinsic dynamics. However, starting from a configuration far from equilibrium, one can study the time dependent behavior of the so-called kinetic Ising model. At zero temperature, the time evolution essentially corresponds to an energy minimizing scheme [5] in the standard rules such as single spin flip Glauber or Metropolis dynamics. The voter model (VM), on the other hand, has no such energy function associated—it is defined by the dynamical rule that an agent follows the state of a randomly chosen neighbor at each time step. The kinetic Ising and voter models are known to be identical in one dimension, while in higher dimensions the dynamical schemes are markedly different [6]. While the coarsening is curvature driven in the Ising model, it is interfacial noise driven in the voter model. This results in different behavior of the relevant dynamical variables such as density of active bonds $n(t)$, persistence probability $P(t)$, and time scales. Active bonds are those which connect neighboring spins with opposite signs. In one dimension, for both the Ising and voter models, $n(t)$ shows power law decay as $t^{-1/2}$. This behavior is true for the Ising model even in higher dimensions. But for the voter model, $n(t)$ asymptotically vanishes as $\frac{1}{\ln t}$ in two dimensions and for dimensions $d > 2$, $n(t) \sim a - bt^{-d/2}$. The dynamics in VM is slower and the consensus time (by consensus we mean the all up and all down absorbing states of the system) typically behaves as $L^2 \log L$ in contrast to L^2 for the IM in two dimensions (L is the system size). The persistence probability $P(t)$, defined as the probability that a spin does not change sign until time t, shows algebraic decay as $t^{-\theta}$ with $\theta = 0.375$ in one dimension [7–10] for the two models. For the IM, $P(t)$ shows algebraic decay even in higher dimensions; in two dimensions $\theta \approx 0.2$ [11–14]. However, for the two-dimensional VM, $P(t)$ has the behavior $\exp[-\text{const}(\ln t)^2]$ [15]. The spin autocorrelation function is another dynamical quantity which again shows different behavior for the VM and the IM in two dimensions [15–19].

Another interesting feature of the Z_2 models (models with spin up and spin down symmetry) with two absorbing states (which are either all spins up or down) is the exit probability $E(\rho)$. $E(\rho)$ is defined as the probability that the final state has all up spins starting with a density ρ of up spins. The exit probability $E(\rho)$ is also different in the two models for $d > 1$. It can be easily argued that in all dimensions, $E(\rho) = \rho$ for the VM. With only nearest neighbor interaction, $E(\rho)$ is obviously linear for the IM also in one dimension. However, allowing further neighbor interactions and other parameters governing the dynamics, a nonlinear behavior can be observed even in one dimension for both the Ising model and the voter model [20–22]. This implies that there is a scope for phenomena like "minority spreading" [23] always in one dimension. In the two-dimensional Ising model $E(\rho)$ shows nonlinear behavior [24] which in the thermodynamic limit approaches a step function. It may be mentioned here that in the zero temperature ordering of Ising model, one encounters the problem of frozen states [25,26]. Hence, the calculation of exit probability is made using only those configurations which reach the all up or all down states.

Since the interfacial noise and surface tension governed dynamics definitely lead to highly different dynamical behavior of several important quantities, it is worthwhile to study models in which both are present in a tunable manner. One such model had been proposed in [27], namely, the generalized voter model. We have, therefore, considered this particular model to study the interplay of the interfacial noise and curvature-driven dynamics.

In the generalized voter model, the dynamical rule has been parametrized so that one can recover a number of models for specific values of the parameters. We have investigated the behavior of the persistence probability, decay of active bonds, exit probability, and time to reach consensus. These quantities are not related in general and hence the effect of changing the parameter values may be different for each of them.

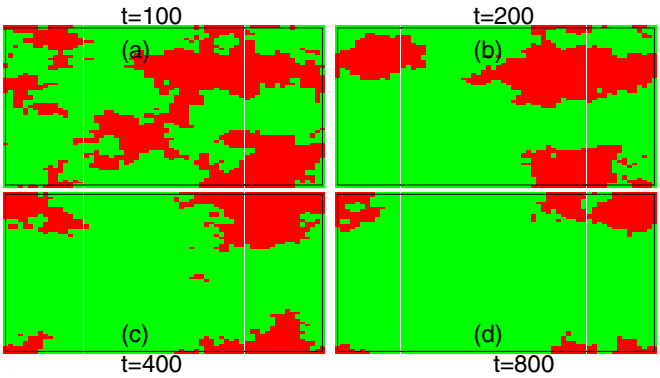

FIG. 1. Typical snapshots at different times for $x = 0.6$ show that coarsening is curvature driven.

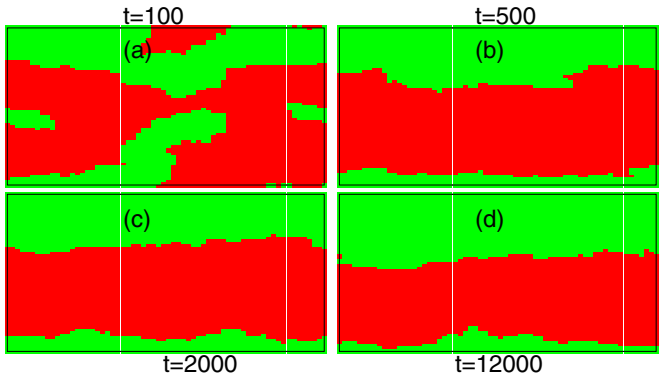

FIG. 2. Certain configurations show very slow relaxation as x is increased. Snapshots show such a configuration for different times for $x = 0.9$.

Let us briefly review the generalized voter model (GVM henceforth) proposed in [27]. Here, at each site of the square lattice there is a spin variable $\sigma_i = \pm 1$. The configuration evolves in time according to single spin flip stochastic dynamics. The spin flip probability $w_i(\sigma)$ for the ith spin is given by

$$w_i(\sigma) = \tfrac{1}{2}[1 - \sigma_i f_i(\sigma)], \tag{1}$$

where $f_i(\sigma) = f(\sum_\delta \sigma_{i+\delta})$, a function of the sum of the nearest neighbor spin variables. The model is defined taking $f(0) = 0$, $f(2) = -f(-2) = x$, and $f(4) = -f(-4) = y$, where x and y are restricted to the conditions $x \leqslant 1$ and $y \leqslant 1$. The original VM is recovered for $x = 0.5$ and $y = 1$, whereas the IM corresponds to $x = 1$, $y = 1$. Along the line $y = 1$, there are two absorbing states: all spins up and all spins down for $x \geqslant 0.5$ (apart from possible frozen states). These states are, however, unstable for $x < 0.5$. As the limiting values $x = 0.5$ and $x = 1.0$ correspond to two different models, one can expect either a sharp transition or a crossover behavior at an intermediate value of x.

We have studied the nonequilibrium behavior and exit probability $E(\rho)$ of the GVM keeping $y = 1$ and varying x using Monte Carlo simulations on $L \times L$ square lattices with $L \leqslant 80$. Periodic boundary conditions have been used and at least 2500 different initial configurations have been simulated. Persistence probability, active bonds dynamics, and consensus times are the quantities estimated. These quantities are unrelated and therefore it is useful to study all of these to check how each of them is affected by tuning of the parameter x.

Snapshots taken during the evolution help in understanding the process quite well. We find that in general for $x > 0.5$, the pictures look very similar to the curvature-driven case. However, for x close to 1, certain configurations show the existence of nearly striped patterns which do reach consensus but very slowly as the interfaces take a long time to vanish. In Figs. 1 and 2, we have shown snapshots for two values of x: for $x = 0.6$, the curvature-driven coarsening is seen to dominate, while for $x = 0.9$ a case is shown where coarsening has led to domains with nearly straight edges prevailing over large time durations. Snapshots for other values of x are given in [28].

The variation of the density of active bonds $n(t)$ against time is plotted in Fig. 3 for different values of x. As x increases from 0.5, we find that $n(t)$ goes to zero involving larger time scales. However, the variation is faster than the $1/\log t$ behavior known for the voter model. It is found that for any $0.5 \leqslant x < 1$ the system always reaches the equilibrium ground state since $n(t)$ vanishes, which implies the freezing probability is zero. Only at $x = 1$ may a frozen state be reached. As x approaches unity (but not equal to it), the initial decay of $n(t)$ can be fitted quite accurately by a power law, while there is a clear crossover to a much slower evolution at later times as shown in the inset of Fig. 3. This suggests that there are two different time regimes. There is an initial time scale up to which the behavior is similar to the Ising model, i.e., $n(t)$ shows a power law decay with exponent close to $1/2$. Beyond this scale, a nonalgebraic slow decay is observed. However, we have checked that the behavior in the latter regime is not like $1/\log t$ as in the voter model but may be even slower than that. For general values of x, we conjecture that at initial times a power law behavior occurs with some correction to scaling as indicated by the plots in Fig. 3; such corrections become weaker as x deviates from 0.5. The second regime with the slower decay exists only for $x > x_c$, $x_c \approx 0.7$. For exactly $x = 1$, the power law behavior is exact before $n(t)$ saturates to a time independent nonzero value due to the frozen stable states.

In order to gain more insight into the dynamical behavior, we have estimated the time τ required to reach the consensus state and its distribution $D(\tau)$. In a detailed study made for

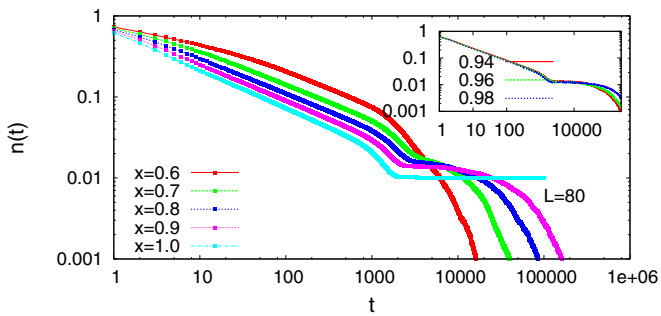

FIG. 3. Plot of density of active bonds with time t for $L = 80$ for $x = 0.6, 0.7, 0.8, 0.9, 1$. The inset shows the variation of active bonds for $x = 0.94, 0.96, 0.98$.

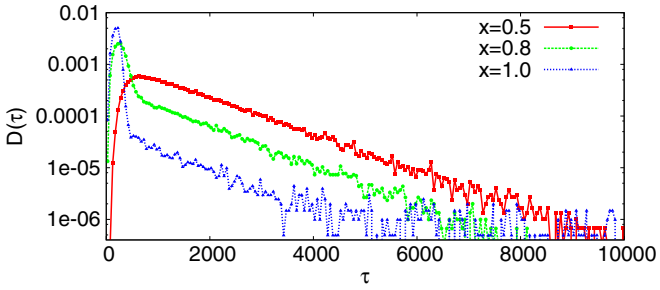

FIG. 4. Plot of distribution of consensus time for $x = 0.5, 0.8, 1$.

$L = 32$, we find that $D(\tau)$ changes its nature remarkably as x is increased (Fig. 4). For $x = 0.5$, $D(\tau)$ shows a conventional behavior; it increases for small τ, and has a broad peak and a long exponential tail. This behavior continues until $x_c \approx 0.70$ beyond which we find that $D(\tau)$ differs considerably for small and large values of τ (see Fig. 8 in the Supplemental Material). Apparently it is an overlap of a symmetric function of finite width peaked about a small value of τ and a slow exponentially decaying function extending to large values of τ (a magnified figure is shown in Fig. 7 in the Supplemental Material). Exactly at $x = 1$, the width of the symmetric function is minimum and the exponential part exists over a much shorter range. We conjecture that in the thermodynamic limit, the exponential part of $D(\tau)$ for $x = 1$ will vanish altogether; this is supported by the data for $L = 64$ (shown in [28]). As the tail of the distribution for any x may be fit by an exponential function $\exp(-\omega\tau)$, one can define a time scale $\tau_{\text{eff}} = 1/\omega$ for each x.

In Fig. 5, we plot the three time scales: τ_{eff}, $\langle\tau\rangle$, and τ_{mp} where τ_{mp} denotes the most probable value. In general, the average values of τ are different from the most probable values. The difference becomes considerable for $x > x_c$ due to the long exponential tails. From Fig. 5 we can conclude that τ_{mp} is very weakly dependent on x; in fact, for $x \geqslant 0.55$, it is almost a constant. On the other hand, the two other time scales are strongly dependent on x; τ_{eff} and $\langle\tau\rangle$ initially decrease and then increase rapidly with x. Evidently, τ_{mp} denotes the time to reach consensus in absence of any intermediate metastable state and is presumably constant for any $x > 0.5$. On the other hand, τ_{eff} corresponds to the time scale associated with the configurations with nearly frozen intermediate states which increase in number as x increases. $\langle\tau\rangle$ shows the increasing trend simply because it is an overall average.

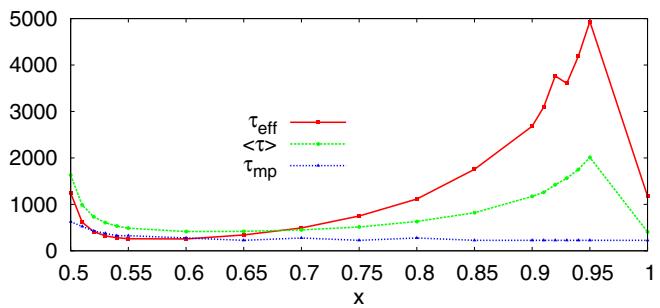

FIG. 5. Plot of different time scales τ_{eff}, $\langle\tau\rangle$, and τ_{mp} as a function of x.

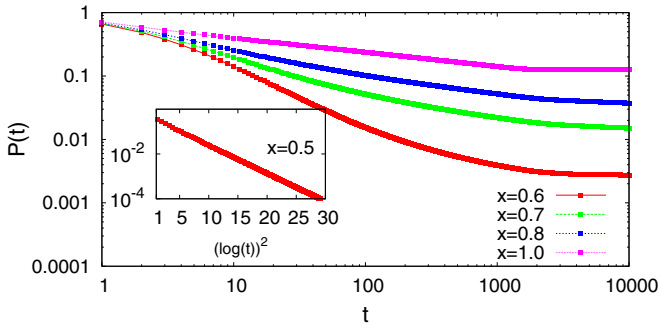

FIG. 6. Plot of persistence probability with time t for $L = 80$ for $x = 0.6, 0.7, 0.8, 1$. The inset shows the variation of $P(t)$ as a function of $(\ln t)^2$ for $x = 0.5$.

The existence of the two different time scales is clearly shown by the above result. The nonmonotonicity in $\langle\tau\rangle$ and τ_{eff} are to be noted; both time scales drop immediately as x deviates from 0.5 and again at $x = 1$. This suggests there are discontinuities at the two well known limiting points.

The average consensus times as a function of the different system sizes apparently show a behavior faster than $L^2 \log L$ for $x > 0.5$. $\langle\tau\rangle$ for other values of L are shown in [28]. The possibility of discontinuities existing at $x = 0.5$ and $x = 1$ is more strongly supported by the data as system size increases. A more conclusive statement about the scaling of the time scales with the system sizes can only be made after a detailed study of the other time scales, which is to be reported later.

We next discuss some other results in the context of the nonequilibrium phenomena. The persistence probability $P(t)$ as a function of time t is plotted in Fig. 6. For $x = 1$, $P(t)$ shows power law decay as $t^{-\theta}$ with $\theta \simeq 0.2$ agreeing with the known result [11–14]. For $x = 0.5$, persistence decays to a very small fraction ($\approx$0) following the behavior $\exp[-0.31(\ln t)^2]$. This behavior is obtained by fitting the data and agrees very well with the form obtained numerically in [15]. For $0.5 < x < 1$, $P(t)$ also approaches a nonzero saturation value; however, there is no clear power law behavior. The saturation value increases with an increase in x in a nonlinear manner.

Lastly we discuss the results for the exit probability (see Fig. 7). The plot of $E(\rho)$ as a function of ρ shows that it is nonlinear except for $x = 0.5$ having strong system size dependence. Different curves intersect at a single point $\rho = \rho_c \simeq 0.5$ (ρ_c should be equal to 0.5 from symmetry argument). The curve becomes steeper as the system size is increased. Finite size scaling analysis as in [29] can be made using the scaling form

$$E(\rho, L) = f\left[\frac{(\rho - \rho_c)}{\rho_c} L^{1/\nu}\right], \tag{2}$$

where $f(y) \to 0$ for $y \ll 0$ and equal to 1 for $y \gg 0$, so that the data for different system sizes L collapse when $E(\rho)$ is plotted against $\frac{(\rho-\rho_c)}{\rho_c} L^{1/\nu}$. The data collapse takes place with $\nu = 1.3 \pm 0.01$ (the unscaled data is shown in the bottom inset) for all values of $x > 0.5$. We conclude that like the Ising model, $E(\rho)$ becomes a step function in the thermodynamic limit. The scaling form given by Eq. (2) is found to fit very

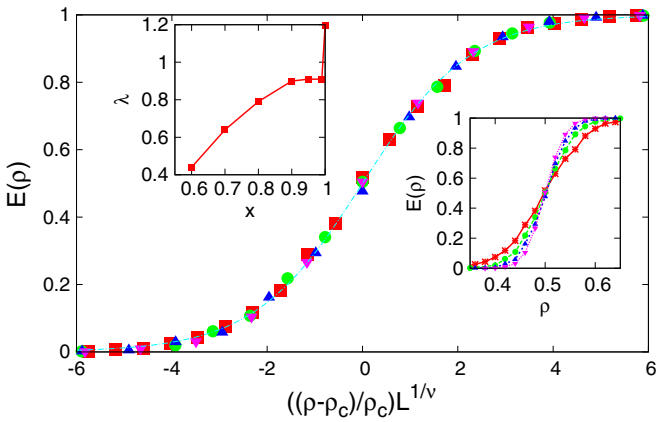

FIG. 7. Data collapse of $E(\rho)$ is plotted against $\frac{(\rho-\rho_c)}{\rho_c}L^{1/\nu}$ for system sizes $L = 32,48,64,80$ for $x = 0.6$. The bottom inset shows the plot of unscaled data against ρ. The top inset shows the plot of λ as a function of x.

well with a general form [29]

$$f(y) = \frac{1 + \tanh(\lambda y)}{2}, \tag{3}$$

where λ depends on x. The dependence of λ on x is shown in the top left inset of Fig. 7. λ which increases with x quantifies the steepness of the $E(\rho)$ curve. λ increases continuously as x is increased from 0.5, consistent with the fact that the $E(\rho)$ should deviate from the linear behavior. However, exactly at $x = 1$, λ increases abruptly to a comparatively larger value indicating a discontinuity.

Let us now discuss the results obtained in this Rapid Communication. First of all it appears that the curvature-driven coarsening governs the dynamics for any $x > 0.5$ at least in the initial stages. This is evident from Fig. 3, which shows that at initial times the ordering becomes much faster compared to the voter model as x is increased from 0.5 (see Fig. 5 in [28]). At the same time, the interfacial noise driven coarsening present in the system, however small, is crucial for leading the system to consensus for larger values of x when the dominant curvature-driven process tends to generate nearly straight interfaces. It is only because of its presence that the freezing probability is zero in the system for any $x \geqslant 0.5$ (but not equal to unity). Thus it is interesting to note that while for smaller values of x the model is closer to the voter model, the average consensus time increases as x approaches unity, the Ising limit. This is apparently counterintuitive as it is known that the evolution in the voter model is slower compared to that in the Ising model in two dimensions. Actually the metastable states increase in number as x is increased (which is not surprising knowing the result for $x = 1$) enabling longer time scales for the system. However, average consensus times are still less than that at $x = 0.5$ up to a certain value of x. Results for different system sizes indicate that this value is very close to x_c (shown in [28]) in the thermodynamic limit, which is consistent with the other results.

The exit probability shows a nonlinear behavior for any $x > 0.5$ with a universal exponent $\nu \approx 1.3$ and a nonuniversal parameter λ entering the scaling function. Since we omit the frozen states for $x = 1$ and the time scales are irrelevant for this measure, it is not surprising that the behavior is Ising like. However, the fact that λ shows a discontinuity at $x = 1$ again shows that the $x = 1$ point has a distinctive feature with respect to the exit probability as well.

In conclusion, quite a few interesting results due to the interplay of the two types of dynamics are obtained in the generalized voter model. The main result is the existence of two time scales in the system for $x > x_c$. One of them, $\tau_{\rm mp}$, is nearly independent of x while $\tau_{\rm eff}$, the other time scale, is a highly nonlinear function of x. Both $x = 0.5$ and $x = 1$ with completely different kinds of dynamical rules have unique features. At $x = 0.5$, $P(t)$ and $E(\rho)$ behave differently compared to any other value of $x > 0.5$; $\langle\tau\rangle$ is discontinuous. On the other hand, $x = 1$ is also unique in the sense that freezing occurs only at this point; $\langle\tau\rangle$ and λ show discontinuity here while well known power law behavior in the relevant quantities exists. The intermediate region $0.5 < x < 1$ does not show any freezing phenomena. Although not algebraic, here $P(t)$ reaches saturation for $0.5 < x < 1$ in contrast to that at $x = 0.5$. No sharp transition is observed for any value of $0.5 < x < 1$, but a crossover behavior at $x = x_c \approx 0.7$ is seen to exist.

P.R. acknowledges financial support from University Grants Commission. P.S. acknowledges financial support from Council of Scientific and Industrial Research project.

[1] T. M. Liggett, *Interacting Particle Systems* (Springer, New York, 1985).
[2] P. L. Krapivsky, S. Redner, and E. Ben-Naim, *A Kinetic View of Statistical Physics* (Cambridge University Press, Cambridge, 2010).
[3] C. Castellano, S. Fortunato, and V. Loreto, Rev. Mod. Phys. **81**, 591 (2009).
[4] P. Sen and B. K. Chakrabarti, *Sociophysics: An Introduction* (Oxford University Press, Oxford, 2013).
[5] R. J. Glauber, J. Math. Phys. **4**, 294 (1963).
[6] I. Dornic, H. Chaté, J. Chave, and H. Hinrichsen, Phys. Rev. Lett. **87**, 045701 (2001).
[7] B. Derrida, A. Bray, and C. Godreche, J. Phys. A **27**, L357 (1994).
[8] B. Derrida, J. Phys. A **28**, 1481 (1995).
[9] B. Derrida, V. Hakim, and V. Pasquier, Phys. Rev. Lett. **75**, 751 (1995).
[10] S. N. Majumdar, Curr. Sci. **77**, 370 (1999).
[11] A. J. Bray, S. N. Majumdar, and G. Schehr, Adv. Phys. **62**, 225 (2013).
[12] B. Yurke, A. N. Pargellis, S. N. Majumdar, and C. Sire, Phys. Rev. E **56**, R40 (1997).
[13] S. N. Majumdar and C. Sire, Phys. Rev. Lett. **77**, 1420 (1996).
[14] T. Blanchard, L. F. Cugliandolo, and M. Picco, J. Stat. Mech. (2014) P12021.
[15] E. Ben-Naim, L. Frachebourg, and P. L. Krapivsky, Phys. Rev. E **53**, 3078 (1996).

[16] D. A. Huse and D. S. Fisher, Phys. Rev. B **35**, 6841 (1987).
[17] H. Takano, H. Nakanishi, and S. Miyashita, Phys. Rev. B **37**, 3716 (1988).
[18] C. Tang, H. Nakanishi, and J. S. Langer, Phys. Rev. A **40**, 995 (1989).
[19] L. Golubović and S. Feng, Phys. Rev. B **43**, 972 (1991).
[20] P. Roy, S. Biswas, and P. Sen, Phys. Rev. E **89**, 030103(R) (2014).
[21] R. Lambiotte and S. Redner, J. Stat. Mech. (2007) L10001.
[22] R. Lambiotte and S. Redner, Europhys. Lett. **82**, 18007 (2008).
[23] S. Galam, Eur. Phys. J. B **25**, 403 (2002).
[24] P. Mullik and P. Sen, Phys. Rev. E **93**, 052113 (2016).
[25] V. Spirin, P. L. Krapivsky, and S. Redner, Phys. Rev. E **63**, 036118 (2001).
[26] V. Spirin, P. L. Krapivsky, and S. Redner, Phys. Rev. E **65**, 016119 (2001).
[27] M. J. de Oliveira, J. F. F. Mendes, and M. A. Santos, J. Phys. A **26**, 2317 (1993).
[28] See Supplemental Material at http://link.aps.org/supplemental/10.1103/PhysRevE.95.020101 for snapshots and other figures and results for $x < 0.5$.
[29] S. Biswas, S. Sinha, and P. Sen, Phys. Rev. E **88**, 022152 (2013).